

Crystal structure of the anticancer drug carmustine determined by X-ray powder diffraction

Carina Schlesinger, Edith Alig, and Martin U. Schmidt ^{a)}

Institute of Inorganic and Analytical Chemistry, Goethe University, Max-von-Laue-Str. 7, 60438 Frankfurt am Main, Germany

(Received 26 February 2021; accepted 26 March 2021)

The structure of the anticancer drug carmustine (1,3-bis(2-chloroethyl)-1-nitrosourea, C₅H₉Cl₂N₃O₂) was successfully determined from laboratory X-ray powder diffraction data recorded at 278 K and at 153 K. Carmustine crystallizes in the orthorhombic space group *P*2₁2₁2₁ with *Z* = 4. The lattice parameters are *a* = 19.6935(2) Å, *b* = 9.8338(14) Å, *c* = 4.63542(6) Å, *V* = 897.71(2) Å³ at 153 K, and *a* = 19.8522(2) Å, *b* = 9.8843(15) Å, *c* = 4.69793(6) Å, *V* = 921.85(2) Å³ at 278 K. The Rietveld fits are very good, with low *R*-values and smooth difference curves of calculated and experimental powder data. The molecules form a one-dimensional hydrogen bond pattern. At room temperature, the investigated commercial sample of carmustine was amorphous. © The Author(s), 2021. Published by Cambridge University Press on behalf of International Centre for Diffraction Data. [doi:10.1017/S0885715621000294]

Key words: structure determination from powder data (SDPD), X-ray powder diffraction, carmustine, Rietveld refinement

I. INTRODUCTION

Carmustine (1,3-bis(2-chloroethyl)-1-nitrosourea, C₅H₉Cl₂N₃O₂, Figure 1, internally called “Carinamustine” due to the name of the first author) is an antineoplastic nitrosourea used in the treatment of several forms of malignant tumors, especially against leukemia and brain tumors (Weiss and Ijssel, 1982; Sarkar *et al.*, 2015; Wang *et al.*, 2017). Carmustine belongs to the nitrosoureas which have the cytotoxic effect of alkylating of the DNA and therefore can decelerate the growth of cancer cells by inhibiting the vital processes such as replication, transcription, and translation of DNA (Hadidi *et al.*, 2019). Since carmustine is highly lipophilic and has a low molecular weight, it easily crosses the blood–brain barrier (Faria *et al.*, 2021).

Carmustine itself is an orange-yellowish powder with a melting point of 304 K. The crystal structure was solved and refined from low-temperature powder diffraction data.

II. EXPERIMENTAL

A. Sample preparation

Carmustine was purchased from Sigma-Aldrich (purity ≥ 98%) and used without further purification or recrystallization.

B. X-ray powder diffraction and data preparation

For the X-ray powder diffraction measurements, the sample was filled into a glass capillary with a diameter of 0.7 mm.

X-ray powder data were recorded at 153 K, at 278 K, at 288 K and at room temperature (298 K) in transmission geometry on a STOE-STADI-P diffractometer equipped with a

curved Ge (111) primary monochromator and a linear position-sensitive detector, using CuKα₁ radiation (λ = 1.5406 Å). A 2θ range of 2.00°–99.99° with a step size of 0.01° was measured. The software WinXPow (Stoe and Cie, 2005) was used for data collection and reduction.

C. Structure solution and refinement

The X-ray powder data of carmustine measured at 153 K were indexed with the program *DICVOL* (Boultif and Louër, 1991). The data were background-corrected using the Chebyshev polynomial as implemented in the program *DASH* (David *et al.*, 2006). The reflection intensities and their correlations were extracted by a Pawley fit (Pawley, 1981) using the program *DASH*. The structure was solved by the real-space method using the simulated annealing approach within *DASH*. The molecular structure was derived from a geometry optimization with the force-field CHARMM (Vanommeslaeghe *et al.*, 2010). In the simulated annealing, no restrictions were placed on the 13 degrees of freedom. The default settings of *DASH* with 25 simulated annealing runs, each with 10⁷ iterations, resulted in a reproducible structure solution. The structure candidate exhibiting the best figure of merit had χ² values of χ²_{prof} = 10.29 and

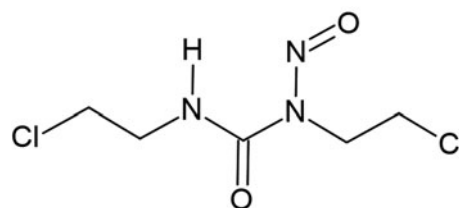


Figure 1. Molecular diagram of carmustine.

^{a)} Author to whom correspondence should be addressed. Electronic mail: m.schmidt@chemie.uni-frankfurt.de

TABLE I. Crystallographic data of carmustine at different temperatures.

Formula	C ₅ H ₉ Cl ₂ N ₃ O ₂	C ₅ H ₉ Cl ₂ N ₃ O ₂
<i>T</i> (K)	153 (−120 °C)	278 (5 °C)
<i>M</i> (g mol ^{−1})	214.05	214.05
Crystal system	Orthorhombic	Orthorhombic
Space group (Nr.)	<i>P</i> 2 ₁ 2 ₁ 2 ₁ (19)	<i>P</i> 2 ₁ 2 ₁ 2 ₁ (19)
<i>a</i> (Å)	19.6935(2)	19.8522(2)
<i>b</i> (Å)	9.8338(14)	9.8843(15)
<i>c</i> (Å)	4.63542(6)	4.69793(6)
α, β, γ (°)	90	90
<i>V</i> (Å ³)	897.71(2)	921.85(2)
<i>Z</i> ; <i>Z'</i>	4; 1	4; 1
<i>D</i> _{calc} (Mg m ^{−3})	1.584	1.542
Radiation; λ (Å)	CuK α ₁ ; 1.5406	CuK α ₁ ; 1.5406
2 θ range (°)	3–99.99	3–99.99
Zero-point error (°)	0.0111(3)	0.0112(3)
<i>B</i> _{iso} (C,N,O)	0.35(4)	2.11(6)
<i>B</i> _{iso} (Cl)	1.21(3)	3.86(4)
<i>B</i> _{iso} (H)	= 1.2* <i>B</i> _{iso} (C,N,O)	= 1.2* <i>B</i> _{iso} (C,N,O)
<i>GOF</i>	1.069	1.053
<i>R'</i> _p (%) ^a	10.550	13.106
<i>R'</i> _{wp} (%) ^a	10.229	11.476
<i>R'</i> _{exp} (%) ^a	9.567	10.901

^aThese values are background-corrected.

$\chi^2_{\text{int}} = 166.05$ (for a χ^2 -value of the Pawley-fit performed with DASH of 2.90).

This structure was subsequently refined by the Rietveld method using the program *TOPAS Academic 4.2* (Coelho, 2018). At first, an additional Pawley fit was performed. The background, described by a Chebyshev polynomial with 20 terms, scale factor, zero-point, lattice parameters, sample parameters, and profile parameters were refined. In the following Rietveld refinement, the atomic positions were refined, too. For the molecular geometry, restraints obtained from the CHARMM force field were applied for bond lengths and bond angles. Preferred orientation was neither observed nor refined. An overall isotropic displacement parameter for all C/N/O atoms was refined. A second isotropic displacement parameter was used for the two chlorine atoms. Hydrogen atoms were included with geometrical restraints and with a displacement parameter 1.2 times larger than that of C/N/O atoms.

In the same way, the crystal structure was again solved and refined from the data measured at 278 K. In this case, the best structure from simulated annealing had figures of merit of $\chi^2_{\text{prof}} = 55.34$ and $\chi^2_{\text{int}} = 1581.57$ for a χ^2 -value of the Pawley-fit performed with DASH of 2.50.

III. RESULTS

At room temperature, the investigated commercial sample of carmustine is a deliquescent to papescant pulp or slurry, which is difficult to handle. The sample was amorphous and did not show any Bragg reflections, neither at room temperature (298 K), nor at 288 K (15 °C). At 278 K (5 °C), the sample was crystalline.

The crystal structure of carmustine was successfully determined from laboratory X-ray powder data recorded at 153 K and at 278 K. The crystallographic data are shown in Table I. The Rietveld refinements converged with excellent *R* values, as well as low *GOF* values. For the 153 K data

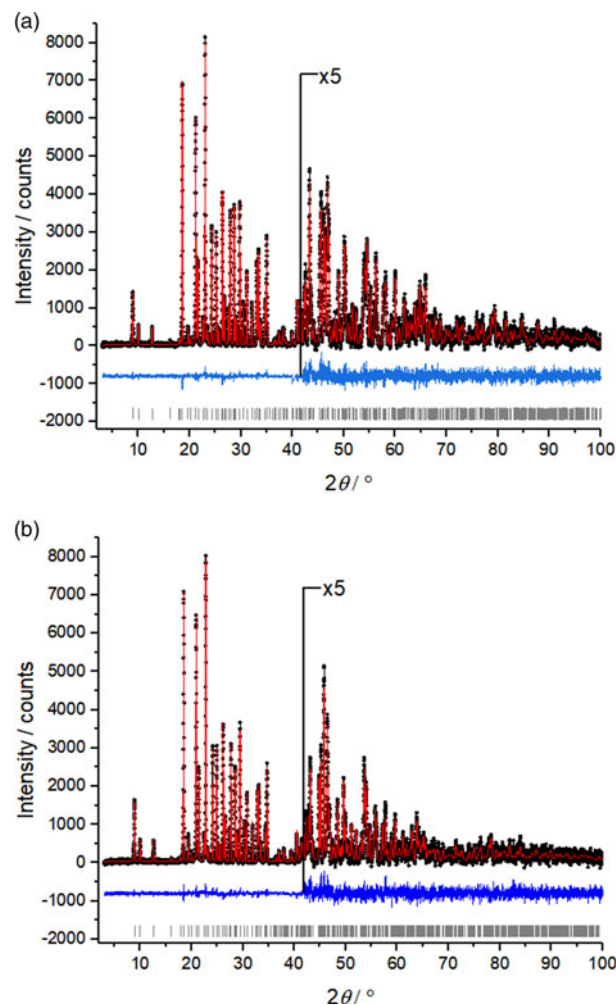


Figure 2. Rietveld plots of carmustine. (a) Data measured at 153 K and (b) data measured at 278 K. Observed intensities are denoted as black dots; calculated intensities as a red line, the difference curve below in blue, and vertical ticks represent the reflection positions.

set, the *GOF* was 1.069 – only 0.002 higher than the *GOF* of the Pawley fit with TOPAS and close to the ideal value of 1.0. The difference curves between experimental and calculated powder data are remarkably smooth for the 153 K data set, as well as for the 278 K data set (Figure 2).

The resulting crystal structure is chemically sensible and exhibits no voids or intermolecular distances that are too close. The bond lengths, bond angles, and torsions angles of carmustine are in good agreement with average values in the Cambridge Structural Database, checked by *Mogul* (Bruno *et al.*, 2004). The molecules are connected by hydrogen bonds and form a chain along the crystallographic *b*-axis [Figure 3(a)]. Neighboring chains are space efficiently stacked along the *c*-direction, resulting in a sheet parallel to (100), see Figure 3(b). These sheets are stacked along [100] and form a dense packing. The Cl atoms of one sheet fill the gaps between the oxygen and chlorine atoms of the neighboring sheet, see Figure 3(a). The intermolecular interactions Cl⋯Cl with a distance of 3.683 Å, and Cl⋯O with a distance of 3.313 Å (at 153 K) are van der Waals interactions. The Cl⋯Cl contacts with angles of $\theta(\text{C}–\text{Cl}\cdots\text{Cl}) = 160.6^\circ$ and $\theta(\text{Cl}\cdots\text{Cl}–\text{C}) = 111.4^\circ$ (at 153 K) are of type II (Sakurai *et al.*, 1963; Gilday *et al.*, 2015). The structure at 278 K is very similar to the structure at 153 K.

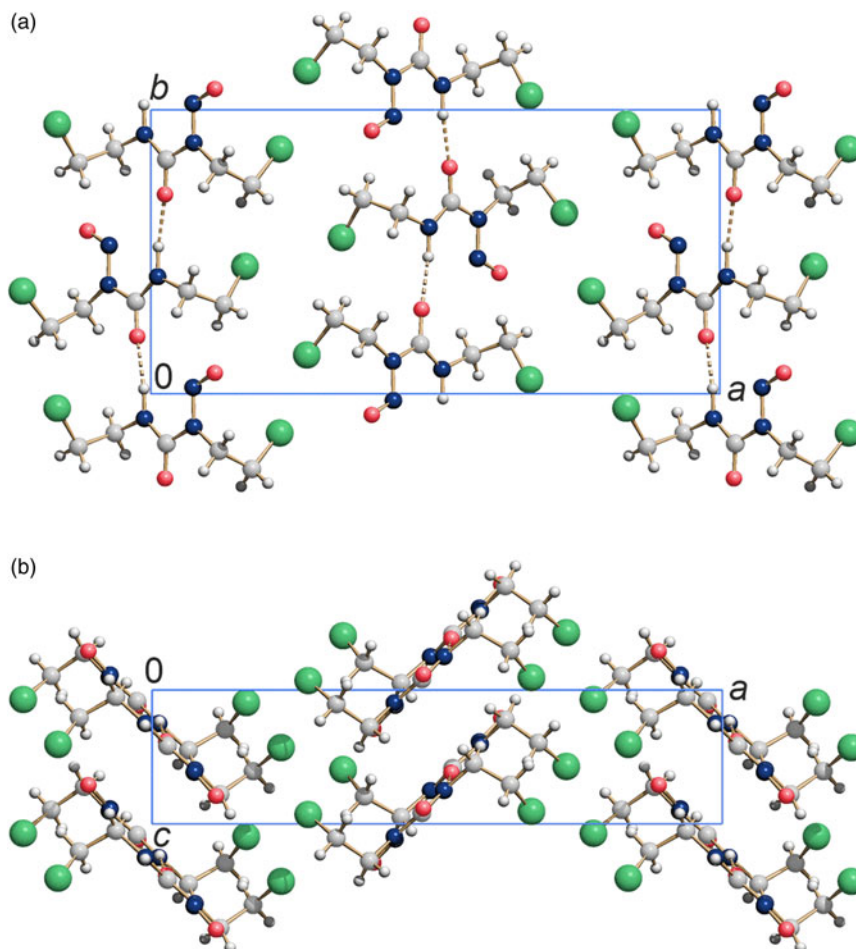


Figure 3. Crystal structure of carmustine at 153 K. (a) View direction [001] and (b) view direction [010]. Colour code: C light gray, O medium red, N dark blue, H small white, Cl large green spheres.

IV. DATA DEPOSITION

The crystallographic data of carmustine are deposited as a crystallographic information file (CIF), including the background-corrected experimental powder profiles, in the Cambridge Structural Database (CSD) with the deposition number 2059041 (153 K data) and 2070329 (278 K data). The original raw data measured at 153 K and 278 K are deposited as files *Carmustine_153K_powder_data.xye* and *Carmustine_278K_powder_data.xye* with the ICDD. The data files can be requested at info@icdd.com.

ACKNOWLEDGEMENTS

The authors are grateful to Lukas Tapmeyer (Goethe University, Frankfurt) for his support with the sample preparation. C. S. acknowledges a grant of the Fonds der Chemischen Industrie.

- Boultif, A. and Louër, D. (1991). "Indexing of powder diffraction patterns for low-symmetry lattices by the successive dichotomy method," *J. Appl. Crystallogr.* **24**, 987–993.
- Bruno, I. J., Cole, J. C., Kessler, M., Luo, J., Motherwell, W. D. S., Purkis, L. H., Smith, B. R., Taylor, R., Cooper, R. I., Harris, S. E., and Orpen, A. G. (2004). "Retrieval of crystallographically-derived molecular geometry information," *J. Chem. Inf. Comput. Sci.* **44**, 2133–2144.
- Coelho, A. A. (2018). "TOPAS and TOPAS-academic: an optimization program integrating computer algebra and crystallographic objects written in C++," *J. Appl. Crystallogr.* **51**, 210–218.

- David, W. I. F., Shankland, K., van de Streek, J., Pidcock, E., Motherwell, W. D. S., and Cole, J. C. (2006). "DASH: a program for crystal structure determination from powder diffraction data," *J. Appl. Crystallogr.* **39**, 910–915.
- Faria, S. H. D. M., Teleschi, J. G., Teodoro, L., and Almeida, M. O. (2021). "Computational investigation of the carmustine (BCNU) alkylation mechanism using the QTAIM, IQA, and NBO models," *Struct. Chem.* **32**, 79–96.
- Gilday, L. C., Robinson, S. W., Barendt, T. A., Langton, M. J., Mullaney, B. R., and Beer, P. D. (2015). "Halogen bonding in supramolecular chemistry," *Chem. Rev.* **115**, 7118–7195.
- Hadidi, S., Shiri, F., and Norouzbazaz, M. (2019). "A DFT study of the degradation mechanism of anticancer drug carmustine in an aqueous medium," *Struct. Chem.* **30**, 1315–1321.
- Pawley, G. S. (1981). "Unit-cell refinement from powder diffraction scans," *J. Appl. Crystallogr.* **14**, 357–361.
- Sakurai, T., Sundaralingam, M., and Jeffrey, G. A. (1963). "A nuclear quadrupole resonance and X-ray study of the crystal structure of 2,5-dichloroaniline," *Acta Crystallogr.* **16**, 354–363.
- Sarkar, A., Karmakar, S., Bhattacharyya, S., Purkait, K., and Mukherjee, A. (2015). "Nitric oxide release by *N*-(2-chloroethyl)-*N*-nitrosoureas: a rarely discussed mechanistic path towards their anticancer activity," *RSC Adv.* **5**, 2137–2146.
- Stoe & Cie (2005). WinXPow. Stoe & Cie, Darmstadt, Germany.
- Vanommeslaeghe, K., Hatcher, E., Acharya, C., Kundu, S., Zhong, S., Shim, J., Darian, E., Guvench, O., Lopes, P., Vorobyov, I., and Mackerell Jr., A. D. (2010). "CHARMM general force field: a force field for drug-like molecules compatible with the CHARMM all-atom additive biological force fields," *J. Comput. Chem.* **31**, 671–690.
- Wang, G.-B., Liu, J.-H., Hu, J., and Xue, K. (2017). "MiR-21 enhanced glioma cells resistance to carmustine via decreasing Spry2 expression," *Eur. Rev. Med. Pharmacol. Sci.* **21**, 5065–5071.
- Weiss, R. B. and Jjssel, B. F. (1982). "The nitrosoureas: carmustine (BCNU) and lomustine (CCNU)," *Cancer Treat. Rev.* **9**, 313–330.